NeuroImage: Clinical 41 (2024) 103570

Contents lists available at ScienceDirect

NeuroImage: Clinical

journal homepage: www.elsevier.com/locate/ynicl

Disrupted third visual pathway function in schizophrenia: Evidence from real and implied motion processing

Antígona Martínez [a,*], Pablo A. Gaspar [b], Dalton H. Bermudez [a], M. Belen Aburto-Ponce [a,c], Odeta Beggel [a], Daniel C. Javitt [c]

[a] Nathan Kline Institute for Psychiatric Research, 140 Old Orangeburg Road, Orangeburg, NY 10962, USA
[b] Department of Psychiatry, Biomedical Neurosciences Institute, IMHAY, University of Chile, Santiago, Chile
[c] Department of Psychiatry, Columbia University Medical Center, New York, NY, USA

A B S T R A C T

Impaired motion perception in schizophrenia has been associated with deficits in social-cognitive processes and with reduced activation of visual sensory regions, including the middle temporal area (MT+) and posterior superior temporal sulcus (pSTS). These findings are consistent with the recent proposal of the existence of a specific 'third visual pathway' specialized for social perception in which motion is a fundamental component. The third visual pathway transmits visual information from early sensory visual processing areas to the STS, with MT+ acting as a critical intermediary. We used functional magnetic resonance imaging to investigate functioning of this pathway during processing of naturalistic videos with explicit (real) motion and static images with implied motion cues. These measures were related to face emotion recognition and motion-perception, as measured behaviorally. Participants were 28 individuals with schizophrenia (Sz) and 20 neurotypical controls. Compared to controls, individuals with Sz showed reduced activation of third visual pathway regions (MT+, pSTS) in response to both real- and implied-motion stimuli. Dysfunction of early visual cortex and pulvinar were also associated with aberrant real-motion processing. Implied-motion stimuli additionally engaged a wide network of brain areas including parietal, motor and frontal nodes of the human mirror neuron system. The findings support concepts of MT+ as a mediator between visual sensory areas and higher-order brain and argue for greater focus on MT+ contributions to social-cognitive processing, in addition to its well-documented role in visual motion processing.

1. Introduction

Schizophrenia (Sz) is a serious mental disorder associated with a range of cognitive impairments predictive of long-term functional and social outcome (Green et al., 2019). The underlying causes are multi-factorial; nevertheless, over recent years dysfunctional auditory and visual sensory processing have become increasingly appreciated as a hallmark of Sz and important contributors to higher-order cognitive impairments (Javitt and Freedman, 2015). In the visual domain impaired motion-perception (e.g. reduced detection sensitivity of moving stimuli) has been linked to impairments in social-cognitive processes including theory of mind (TOM) (Kelemen et al., 2005), biological-motion perception (Okruszek and Pilecka, 2017) and face emotion recognition (FER) (Martinez et al., 2018; Martinez et al., 2019). These findings are consistent with the recent proposal of the existence of a specific visual pathway specialized for social perception (Pitcher and Ungerleider, 2021) in which motion is a fundamental component. This 'third visual pathway', located at the lateral surface of the brain, runs from primary visual cortex (V1) through visual motion-processing regions located in middle temporal cortex (MT+), to the superior temporal sulcus (STS), an area known to respond to biological motion and a variety of dynamic social cues including faces and bodies (Allison et al., 2000; LaBar et al., 2003).

In Sz, functional magnetic resonance imaging (fMRI) studies have revealed altered activation patterns in third visual pathway regions, especially STS, during TOM (reviewed in Kronbichler et al., 2017), FER (Martínez et al., 2022; Mier et al., 2017) and biological motion perception (Matsumoto et al., 2018) tasks. Additionally, activation of MT+ in response to simple moving stimuli (Chen et al., 2008; Lencer et al., 2005; Martinez et al., 2018; Martinez et al., 2019; Scheliga et al., 2022), in parallel with aberrant interactions involving V1 and the pulvinar nucleus of the thalamus (PulN), (Martinez et al., 2018; Martínez et al., 2022) has also been reported.

The sensitivity of MT+ is not limited to real physical motion but extends also to the representation of *implied-motion* derived from static images containing cues conveying information about an objects' motion direction and speed (Fawcett et al., 2007; Kourtzi and Kanwisher, 2000; Osaka et al., 2010; Senior et al., 2000; Zeki et al., 1993). The

* Corresponding author.
E-mail addresses: martinez@nki.rfmh.org (A. Martínez), Odeta.Beggel@nki.rfmh.org (O. Beggel).

https://doi.org/10.1016/j.nicl.2024.103570
Received 31 August 2023; Received in revised form 17 December 2023; Accepted 23 January 2024
Available online 26 January 2024

involvement of MT+ during implied-motion perception has been attributed to activity of the mirror neuron system (MNS) (Filimon et al., 2007; Proverbio et al., 2009; Urgesi et al., 2006). Mirror neurons, originally discovered in macaques, discharge during both active execution and passive observation of a motor act, thereby "mirroring" the goal-directed actions of others (reviewed in Bonini et al., 2022). In addition to action observation and imitation, the human MNS is hypothesized to play a central role in social cognitive processes such as TOM, empathy, and FER (Schmidt et al., 2021).

FMRI studies have consistently identified a set of 'core' regions within premotor, inferior frontal and parietal cortex that comprise the putative human MNS. A more extended network of cortical and subcortical areas also showing enhanced activation during action observation and imitation have also been identified as having mirror properties. These include the middle frontal gyrus (MFG), sensorimotor cortex (SMC), supplementary motor area (SMA), posterior superior temporal sulcus (pSTS) and the putamen (Bonini, 2017; Caspers et al., 2010; Errante and Fogassi, 2020; Ferrari et al., 2017; Molenberghs et al., 2012). Disrupted MNS activity during action observation/imitation has been reported in several neuropsychiatric disorders (reviewed in Chan and Han, 2020; Jeon and Lee, 2018) including Sz (Brown et al., 2016; Mehta et al., 2014b; Thakkar et al., 2014; Valizadeh et al., 2022). In Sz, altered MNS activity has also been associated with impaired TOM performance (Choe et al., 2018) and greater symptom severity (Mehta et al., 2014a; Saito et al., 2018; Schilbach et al., 2016).

In this study, we investigated whether reported MT+ deficits to explicit motion in Sz would carry forward to the processing of static, implied-motion stimuli shown previously to engage the MNS (Proverbio et al., 2009; Urgesi et al., 2006) and if so, would these MT+ deficits mediate impairments within higher-tier social cognitive regions such as pSTS. We used naturalistic stimuli that either contained real-motion (video clips) or in which motion, or its absence, were implied by static photographs (Fig. 1**A**). Prior behavioral studies have investigated patients' ability to extrapolate the implied trajectory of a "freeze-frame" picture (Jarrett et al., 2002), to our knowledge, however, the involvement of MT+ in implicit motion processing has not been investigated previously in Sz.

We hypothesized that, relative to control participants, Sz patients would show diminished MT+ activation to both real- and implied-motion stimuli and that significant correlations would be observed across stimulus types, arguing for intrinsic dysfunction of MT +. Further, based on our previous studies (Martinez et al., 2019; Martínez et al., 2022) we additionally hypothesized that MT+ deficits in Sz to explicit (real) motion would be associated with altered responses within early visual areas (e.g. V1) whereas deficits in response to stimuli with implied-motion would be associated with dysfunction of high-order cortical areas comprising the MNS.

Finally, while the majority of studies of cognitive impairment in Sz focus on cortical activations, it is increasingly appreciated that the network structure of the brain is coordinated extensively through subcortical regions including thalamus and basal ganglia, which participate in canonical resting-state networks (Choi et al., 2012; Ji et al., 2019; Zhang et al., 2008). Thus, in the present study we additionally investigated functioning of subcortical regions implicated in real- and implied-motion processing.

2. Materials and methods

2.1. Participants

Participants were 28 individuals meeting DSM-IV criteria for Sz assessed by the Structured Clinical Interview for DSM-IV (SCID) (First et al., 1997) and 20 demographically-matched NT controls with no history of SCID-defined axis I psychiatric disorders. Controls were recruited from the volunteer recruitment pool at the Nathan Kline Institute for Psychiatric Research (NKI). Sz participants were recruited from outpatient and chronic inpatient clinics in the New York City area and were on stable doses of antipsychotics at time of testing. Chlorpromazine-equivalents (CPZ-equivalents) were estimated as described previously (Andreasen et al., 2010) **(**Table 1).

Participants were excluded if they had neurological or ophthalmologic disorders or if they met criteria for alcohol/substance dependence within the last 6 months or alcohol/substance abuse within the last month. All subjects provided written informed consent after study procedures were fully explained. All procedures were approved by the Nathan Kline Institute/ Rockland Psychiatric Center Institutional Review Board in accordance with The Code of Ethics of the World Medical Association (Declaration of Helsinki) for experiments involving humans.

In Sz, symptoms were assessed using the Positive and Negative Symptom Scale (PANSS). Neurocognitive performance was assessed using the Processing Speed Index (PSI) and Perceptual Organization Index (POI) of the WAIS-4. Estimated premorbid IQ was assessed using the Quick IQ test (Ammons and Ammons, 1962).

The Penn Emotion Recognition (ER-40) test (Taylor and MacDonald, 2012) was administered to all participants to ascertain FER accuracy.

Individual thresholds for coherent-motion detection were determined using random-dot kinematograms as described previously (Martinez et al., 2018). Analyses were carried out on motion-sensitivity scores, calculated as 1 over the estimated coherence threshold for each participant.

2.2. Task design

Stimuli depicted animals in the wild or humans performing a sports activity. For each stimulus category, three stimulus types were used: 1) black and white video clips containing real-motion; 2) greyscale photographs depicting implied-motion; and 3) greyscale photographs depicting motion-absence (Fig. 1**A**). Implied-motion stimuli were single frames captured from real-motion videos. No-motion images were chosen to match real- and implied-motion stimuli. All images were matched for luminance and contrast using the SHINE toolbox (Willenbockel et al., 2010). All stimuli subtended 8.5° × 8.5°.

Stimuli were delivered in 24-second blocks. During real-motion blocks, eight unique 3-second video clips were presented with no break between clips. In implied- and no-motion blocks, eight unique images were presented for 2.5-seconds followed by a 0.5-second interstimulus interval. Stimulation blocks were interleaved with 12-second 'rest' blocks (fixation alone). A total of 12 blocks (four each of real-, implied- or no-motion) were delivered in random order in each of two fMRI scans. Half of the blocks consisted of animal stimuli, half of sports. During scanning, participants monitored a central fixation cross and responded by button-press upon detection of its occasional dimming occurring every 3–9 s.

2.3. Data acquisition and pre-processing

FMRI data were collected on a Siemens 3 T TIM-Trio scanner. At least one high-resolution structural image was acquired per participant using a Magnetization-Prepared Rapid Gradient-Echo (MP-RAGE) sequence (spatial resolution = 1 mm isotropic, repetition time (TR) = 2000 ms; echo time (TE) = 3.5 ms; flip angle 8°, 192 slices). Echo-planar images (EPIs) (2.5 mm isotropic, TR = 2000 ms, TE = 30 ms, flip angle 80°) were acquired on 36 contiguous slices in the axial plane.

Functional data were preprocessed and analyzed using a combination of Analysis of Functional NeuroImages (AFNI) (Cox, 1996), Surface Mapping (SUMA) (Saad and Reynolds, 2012). Preprocessing consisted of concatenating data from two runs, removal of signal deviation > 2.5 SDs from the mean (3dDespike), temporal alignment, identification of motion outliers per run and scaling of blood-oxygen-level-dependent (BOLD) values to mean percent signal change (Taylor et al., 2018). Cortical data was spatially smoothed with a 6 mm full-width-at-half-maximum Gaussian kernel.

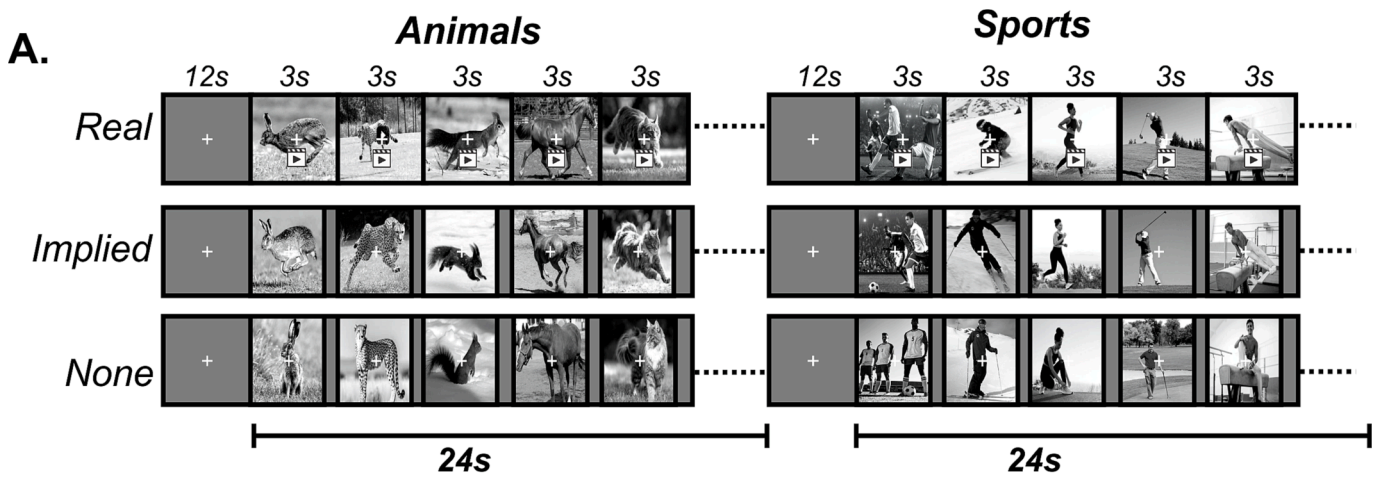

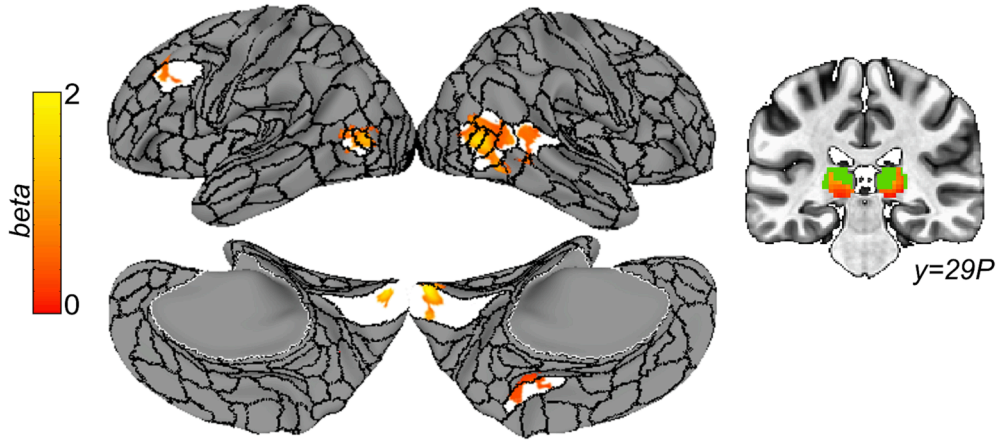

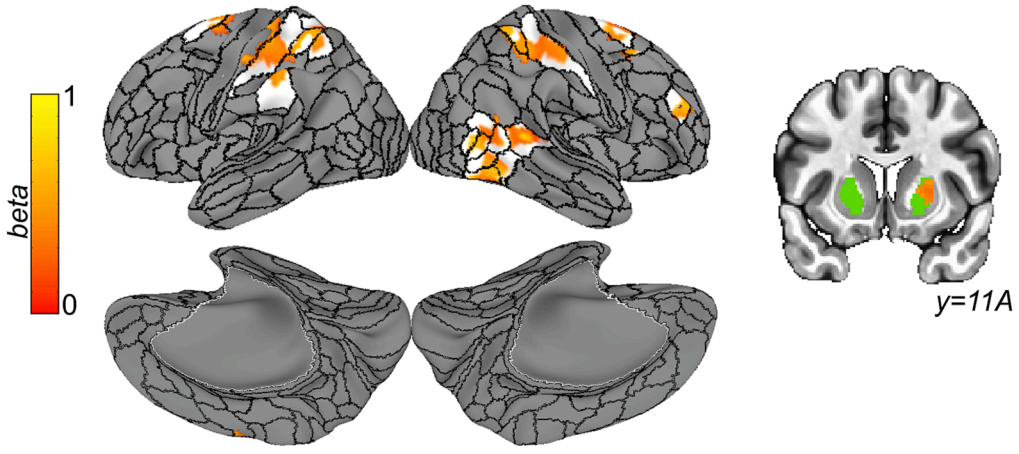

(caption on next page)

Fig. 1. A) Examples of 'Animal' (left) and 'Sports' (right) stimuli. Stimuli were delivered in 24-second stimulation blocks interleaved with 12-second blocks of fixation only. In all cases the stimuli were either: (*top row*) Eight unique video clips depicting motion, lasting 3 s each; (*middle row*): Eight static images, (single frames from videos), suggesting implied motion; or (*bottom row*) Eight static images, matched to the motion/implied motion images, but depicting static scenes without motion. Static images (both implied and no-motion), were displayed for 2.5 s, followed by a 0.5-second interstimulus interval (ISI). A central fixation cross was present throughout, and participants were instructed to press a button when the cross dimmed in luminance. B) Whole-brain cortical activation ($p < 0.05$, adjusted) for the real-motion versus no-motion contrast across participants. Activation maps are superimposed on the HCP-MMP1.0 atlas. Parcels corresponding to regions with significant clusters of activation are colored white. Group-level subcortical activation in the pulvinar is shown on right on a posterior coronal slice (y = -29), displayed against the anatomical pulvinar mask in green. In all activation maps, color scale represents associated beta parameter values. **C)** As above for the implied-motion versus no-motion contrast. Group-level activation within the putamen, overlaid on the basal ganglia anatomical mask (in green) shown on an anterior coronal slice (y = 11). (For interpretation of the references to color in this figure legend, the reader is referred to the web version of this article.)

Table 1
Demographic, clinical and behavioral characteristics. Neurotypical (NT) and schizophrenia (SZ) participants differed in terms of years of education, processing speed (PSI) and perceptual organization (POI) index scores.

	NT ($n = 20$)	SZ ($n = 28$)	Difference
Age	35.5 (9.4)	38.8 (10.1)	t(46) = -1.15, p =.25
Sex (F/M)	4/16	8/20	$x^2 = 0.45$, p =.49
Quick IQ	99.9 (8.3)	98.1 (9.3)	t(46) = 0.69, p =.49
Years of Education	14.7 (2.1)	11.9 (1.9)	*t(46) = 4.76, p <.001*
Participant SES	42.7 (10.9)	25.0 (6.2)	*t(46) = 7.11, p <.001*
Parental SES	42.5 (14.4)	37.5 (12.7)	t(46) = 1.17, p =.25
PSI	100.1 (11.0)	83.7 (11.3)	*t(46) = 4.89, p <.001*
POI	108.9 (15.9)	93.4 (18.3)	*t(46) = 2.98, p =.005*
Illness Duration (yrs)	–	14.2 (9.1)	–
Edinburgh Score	15.7 (6.6)	16.9 (5.4)	t(46) = -0.69, p =.49
CPZ Equiv. (SZ)	–	834.8 (629.1)	–
Anti-Psychotic		Typical (6)	–
		Atypical (15)	–
		Combination (7)	–
ER-40	35.8 (1.9)	28.7 (5.6)	*t(46) = 5.56, p <.001*
Motion Sensitivity	10.9 (4.2)	7.3 (3.0)	*t(46) = 3.41, p =.001*
PANSS (positive)	–	11.1 (4.1)	–
PANSS (negative)	–	19.3 (5.6)	–

Participant, but not parental, socioeconomic status (SES) was also significantly lower in the SZ group. Behavioral measures of face-emotion recognition, (derived from the Penn Emotion Recognition Task, ER-40) and motion sensitivity scores, calculated as 1/threshold from the coherent motion detection task, were additionally lower in SZ compared to NT participants. CPZ: Chlorpromazine equivalents; PANSS: Positive and Negative Syndrome Scale. Standard deviations in parentheses.

For each participant, the cortical surface was rendered using FreeSurfer's (Version 7.2.0, FreeSurfer.net) 'reconall' command and standard preprocessing steps including motion correction, removal of non-brain tissue, skull-stripping, segmentation of white and gray matter and intensity normalization.

Analyses were carried out on the gray-matter ordinates of each individual cortical surface aligned to the FreeSurfer (fsaverage)141-standard mesh. Cortical data was sampled to the Human Connectome Project multimodal cortical parcellation atlas (HCP-MMP1.0) (Glasser et al., 2016), resampled to fsaverage. The HCP atlas subdivides the brain into 180 regions (parcels) per hemisphere based on functional and structural properties. For subcortical structures, parallel analyses were carried out in volumetric space registered to the MNI-152 template brain.

2.4. fMRI data analysis

For each participant, a general linear model (GLM), implemented in AFNI's *3dDeconvolve*, was used to estimate beta parameter values across the whole brain for each stimulus type (real-, implied-, no-motion). Regressors were constructed by convolving a gamma-variate function with a boxcar function corresponding to the timing of stimulation blocks. Six motion parameters (three translation and three rotation parameters per frame) as well as white matter (WM) and cerebrospinal fluid (CSF) signal time series were included in the GLM as nuisance regressors.

To avoid potential issues related to circularity in analyses of group differences (Kriegeskorte et al., 2009), an analysis of variance (ANOVA) was first conducted across all participants (*3dANOVA*). Cluster size threshold corresponding to a family-wise error rate of $\alpha < 0.05$ were calculated using Monte Carlo simulations (*slow_surf_clustsim.py)*. The resulting groupwise maps were overlaid onto the HCP atlas to identify and combine parcels that exhibited significant activation across the NT and Sz groups. The aggregated parcel maps were subsequently utilized as masks in subsequent between-group analyses.

Differences between groups in response to both real-motion and implied-motion stimuli were assessed by repeated-measures ANOVA (*3dMVM*) using individual beta parameter maps with stimulus type (real-, implied-, no-motion) as a within-group factor, and group membership (NT, Sz) as the between-group factor. The GLM also included two general linear tests for the contrasts of real- versus no-motion and implied- versus no-motion stimuli. Voxel-level false discovery rate (FDR) was used to correct for multiple testing using *3dFDR* and statistical significance set at adjusted $p < .05$.

Mean activation values (beta coefficients) were extracted from the corresponding HCP parcels that demonstrated significant group differences in the linear contrast maps. These extracted values were used in subsequent between-group ANOVAs. Effect sizes were calculated using Cohen's d. All statistical tests were two-tailed, and, where appropriate, included participant sex, age, and IQ as covariates.

In addition, group differences were evaluated from within two a-priori identified subcortical regions of interest (ROIs), the PulN and basal ganglia (caudate, putamen and globus pallidus) identified anatomically using a template mask in standard MNI space.

2.5. Correlation and mediation analyses

In post-hoc tests, mean beta values for the contrasts of real-motion and implied-motion versus no-motion were extracted. These values were used in both correlation and exploratory mediation analyses. To investigate the interrelationships between MT+ activation and other regions exhibiting group differences during real- and implied-motion processing, Pearson's partial correlation was employed with participant age, sex, IQ, and group membership as covariates. To correct for multiple testing, p-values were adjusted using the False Discovery Rate (FDR) method.

Mediation analyses were carried out using SPSS 26.0 (https://www.ibm.com/products/spss-statistics), employing the PROCESS macro (version 4.2) (Hayes, 2013). A three-variable path model (model 4) was used to explore the potential mediating role of MT+ in the context of real- and implied-motion processing. To assess the statistical significance of the indirect pathways, indicative of mediation effects, a non-parametric bootstrap method was used involving 10,000 replication samples to obtain a 95 % confidence interval (CI) (Preacher and Hayes, 2008). Mediation effects were deemed statistically significant if the bootstrapped 95 % CI did not encompass zero.

3. Results

3.1. Behavioral measures

As expected, both motion-sensitivity ($F(1,43) = 9.48$, $p = .004$, $d =$

1.00) and FER (Penn ER-40) ($F(1,43) = 28.39$, $p < .001$, $d = 1.63$) scores were significantly lower in Sz relative to NT individuals (Table 1).

3.2. Whole-brain groupwise analyses

Significant groupwise activations ($p < .05$, adjusted) elicited during blocks of 1) real-motion clips, 2) static images with implied-motion and 3) static images with no-motion, relative to fixation blocks, are shown in Supplementary Fig. 1.

Images depicting no-motion elicited activation in a total of 14 bilateral parcels located primarily within the primary visual cortex (V1), early visual areas (V2,V3,V4), and ventral-occipital cortex (PIT, PH, VMV3,V4t, V3CD, VVC). Mean beta value was extracted individually from each parcel and entered into repeated measures ANOVA. Across parcels, activation was equivalent in NT versus Sz groups ($F(1,43) = 0.82$, $p = .37$) (Supplementary Table 1). Thus, to evaluate real- and implied-motion processing, all further analyses were calculated relative to the no-motion condition.

When contrasted to no-motion stimuli, real-motion stimuli elicited significant activation ($p < .05$, adjusted) across all participants in regions associated with the third visual pathway, specifically V1, MT+ (parcels MT, MST), and pSTS (TPOJ1, TPOJ2). Beyond these areas, significant activation was also observed in several other regions, including the posterior cingulate cortex (5mv), middle frontal cortex (8c), lateral occipital cortex (LO3), and inferior temporal cortex (FST). In total, these activations spanned 9 cortical parcels in the right hemisphere (RH) and 4 parcels in the left hemisphere (LH), (Fig. 1**B,** Supplementary Table 2). Additionally, significant subcortical activation of bilateral PulN was observed.

Similar to the real-motion contrast, the contrast of implied- versus no-motion stimuli elicited activation in MT+ and pSTS of the RH across all participants. Additionally, a network of fronto-parieto-temporal regions typically associated with the human MNS, was activated. This network included areas in the middle frontal cortex (i6-8), dorsolateral prefrontal cortex (p9-46v; DLPFC), and parts of sensorimotor (2; SMC), supplementary motor (6ma), inferior parietal (PF, IP0), and superior parietal (SPL; 7AL, 7PC) cortex. Overall, these activations spanned 14 parcels in the RH and 6 in the LH. The RH putamen nucleus of the basal ganglia was also significantly activated across all participants (Fig. 1C, Supplementary Table 3).

The composite of parcels identified in both groupwise contrasts above *(*Fig. 1**B, 1C in white***)** were used as masks in subsequent analysis of group differences.

3.3. Group Differences: Real-motion contrast

Compared to NT participants, mean activation within parcels comprising the third visual pathway (V1, MT+, pSTS) was significantly reduced in Sz in the contrast of real- versus no-motion stimuli (Fig. 2**A,** Table 2 **top**). In V1 ($F(1,43) = 9.92$, $p = .003$, $d = 0.84$) and MT+ ($F(1,43) = 12.05$, $p = .010$, $d = 0.85$) these reductions were observed bilaterally but in both cases the main effect of hemisphere (V1: $F(1,43) = 0.04$, $p = .834$; MT+: $F(1,43) = 3.77$, $p = .060$) as well as the hemisphere x group interaction (V1: $F(1,43) = 2.43$, $p = .126$; MT+: $F(1,43) = 0.21$, $p = .652$) was non-significant. Thus, in subsequent analyses, beta parameters for V1 and MT+ were averaged across hemispheres.

Other cortical regions active across participants did not show significant group differences (Fig. 2**A** in white; Supplementary Table 2).

Subcortically, activation within bilateral PulN was significantly lower, overall, in Sz compared to NT participants ($F(1,42) = 8.63$, $p = .005$, $d = 0.93$) with no effect of hemisphere ($F(1,42) = 0.24$, $p = .63$) or group x hemisphere interaction ($F(1,42) = 0.06$, $p = .81$) **(**Fig. 2**B).** Mean PulN activation was used in subsequent analyses.

3.4. Group Differences: Implied-motion contrast

Mirroring the effects observed in the real-motion contrast, activation of regions constituting the third visual pathway (MT+, $F(1,43) = 5.90$, $p = .019$, $d = 0.76$; pSTS, $F(1,43) = 12.30$, $p = .001$, $d = 0.97$) was significantly reduced in the Sz group in the implied- versus no-motion contrast (Fig. 2**C**). Moreover, the reductions in both MT+ ($r_p = .41$, $p = .004$) and pSTS ($r_p = .48$, $p = .001$) were significantly correlated with the diminished activations observed in these same regions during real-motion processing.

Significantly reduced activations in Sz relative to NT participants were also found within regions associated with the human MNS including SMC ($F(1,42) = 8.93$, $p = .004$, $d = 1.25$), SPL ($F(1,43) = 4.08$, $p = .045$, $d = 0.79$) and DLPFC ($F(1,42) = 4.93$, $p = .032$, $d = 0.82$) (Table 2 **bottom).** In all cases, group differences were only significant in the RH.

Several other regions comprising the MNS, including supplementary motor and inferior parietal cortex, showed equivalent activation in both NT and Sz participants (Fig. 2**C** in white; Supplementary Table 3).

Finally, Sz participants also showed reduced activation subcortically in the putamen of the RH ($F(1,42) = 4.23$, $p = .046$, $d = 0.74$) (Fig. 2**F,** Table 2 bottom).

3.5. MT+ intercorrelations and mediation

To investigate the role of MT+ on the perception of real- and implied-motion, we performed partial correlations between MT+ activation in the real- and implied-motion contrast and activation of all other brain regions showing significant group-related differences. Group membership, sex, age and IQ were controlled for and the resulting p-

Table 2
Mean activation (beta parameter estimates) for neurotypical (NT) and schizophrenia (SZ) groups within brain regions showing significant group differences during the processing of real-motion (top panel) and implied-motion (bottom panel).

	Real Motion			No Motion			Real vs. No Motion		
Region	*(NT/SZ)*	*t(46)*	*Adj. p*	*(NT/SZ)*	*t(46)*	*Adj. p*	*(NT/SZ)*	*t(46)*	*Adj. p*
MT+	1.32/1.01	*2.61*	*0.012*	0.33/0.49	*−1.41*	0.166	0.99/0.53	*2.91*	*0.006*
V1	0.76/0.46	2.08	0.026	0.40/0.62	−1.32	0.263	0.36/-0.16	2.86	*0.006*
pSTS	0.64/0.43	*2.67*	*0.010*	0.07/0.15	*−1.11*	0.274	0.65/0.28	*3.26*	*0.002*
PulN	0.47/0.026	*3.05*	*0.004*	0.06/0.09	*−0.30*	0.766	0.41/-0.066	*3.16*	*0.003*
	Implied Motion			**No Motion**			**Implied vs. No Motion**		
Region	***(NT/SZ)***	***t(46)***	***Adj. p***	***(NT/SZ)***	***t(46)***	***Adj. p***	***(NT/SZ)***	***t(46)***	***Adj. p***
MT+	0.80/0.55	2.03	*0.048*	0.33/0.49	−1.41	0.166	0.47/0.06	2.61	*0.006*
pSTS	0.33/0.11	2.23	*0.030*	0.07/0.15	*−1.11*	0.274	0.34/-0.05	3.30	*0.002*
SPL	0.20/0.01	2.13	*0.038*	−0.14/0.06	−1.54	0.130	0.34/-0.05	2.69	*0.010*
SMC	0.26/0.11	2.16	*0.035*	-0.09/0.12	−2.62	0.011	0.35/-0.01	4.28	*<0.001*
DLPFC	0.49/0.22	2.30	*0.026*	0.12/0.22	−0.96	0.353	0.32/-0.05	2.99	*0.004*
Putamen	0.22/0.07	1.80	*0.070*	-0.10/-0.02	−0.96	0.343	0.32/0.08	2.51	*0.015*

Mean values and False Discovery Rate (FDR)-adjusted p-values (Adj. p) for activations elicited by real-, implied- and no-motion stimuli, as well as the contrasts between real/implied-motion and no-motion stimuli are given.

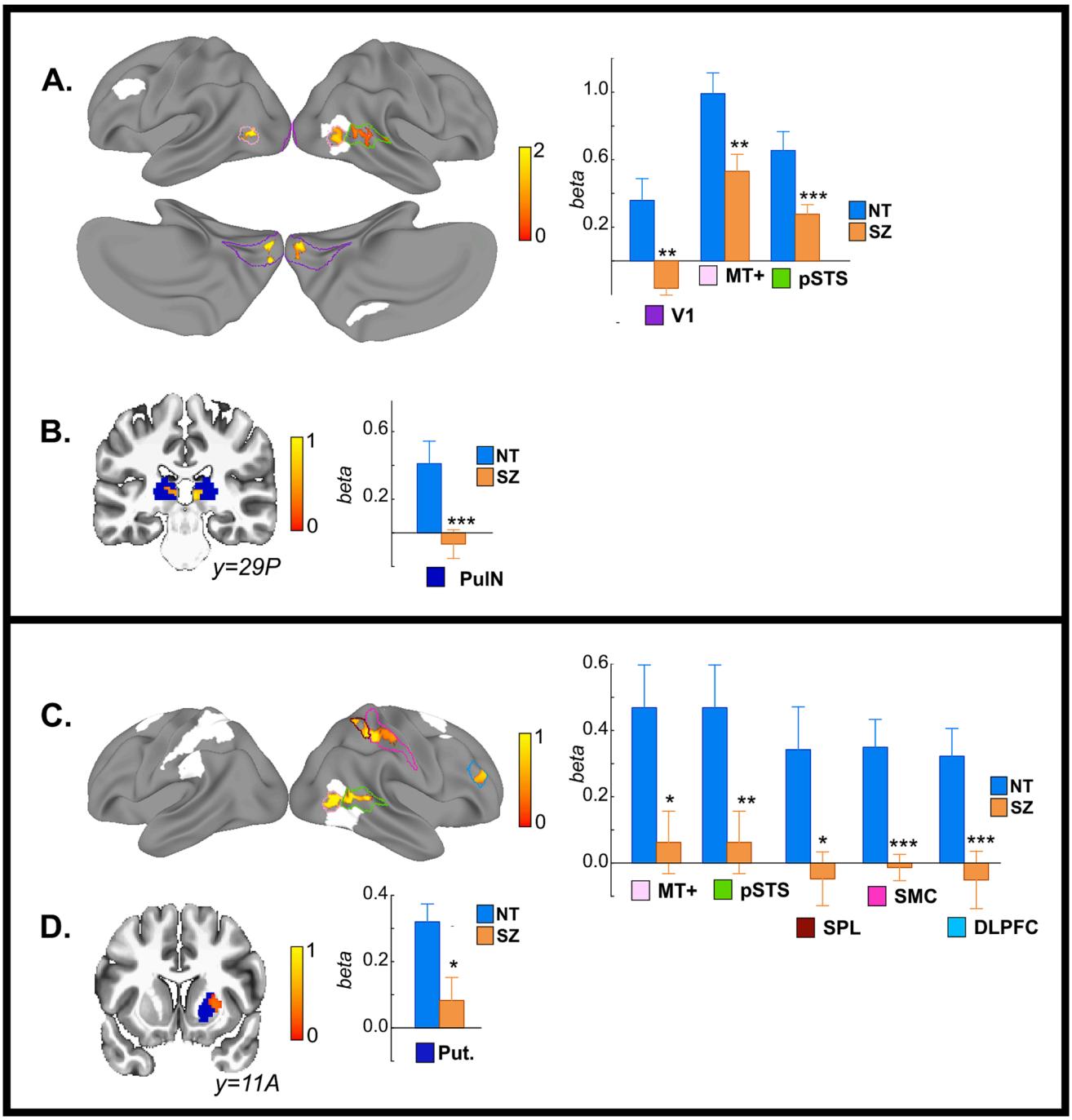

Fig. 2. A) Regions with significant (p <.05, adjusted) group differences elicited by the contrast of real-motion versus no-motion stimuli, shown within colored outlines of corresponding HCP parcels (V1: purple, MT+: pink, posterior superior temporal sulcus, pSTS: green). Filled white parcels showed equivalent activation in the schizophrenia (SZ) and neurotypical control (NT) groups. Bar graphs are of mean activation (beta values) extracted from each parcel for NT (blue) and SZ (orange) participants. B) Significant group differences in the real-motion contrast within bilateral pulvinar (PulN) and bar graphs of mean activation extracted from the anatomical mask (in blue) used for analyses. C) Cortical areas with significant group differences in the implied-motion contrast and bar graphs of mean beta values extracted from each corresponding HCP parcel. In addition to MT+ and pSTS, differences were observed within parcels in the superior parietal lobe (SPL, red outline), sensorimotor cortex (SMC, dark pink) and dorsolateral prefrontal cortex (DLPFC, light blue). D) Significant group differences in activation elicited by the contrast of implied- versus no-motion stimuli within the putamen (Put.). Bar graphs are mean activation (beta values) extracted from the analysis mask (blue). Significance values are denoted as: *, p <.05; **, p <.01; ***, p <.001). (For interpretation of the references to color in this figure legend, the reader is referred to the web version of this article.)

values were adjusted using FDR correction based on three correlations for real-motion (pSTS, V1, PulN) and five correlations for implied motion (pSTS, SPL, SMC, DLPFC and putamen).

In the real-motion condition, MT+ activation was significantly correlated with activation of pSTS (r_p =.54p <.001) (Fig. 3**A**), V1(r_p =.45p =.003) (Fig. 3**B**), and PulN (r_p =.51p <.001) (Fig. 3**C**). Similarly, for the implied-motion contrast, MT+ and pSTS activation were significantly correlated (r_p =.55p <.001) (Fig. 3**D**), as were MT+ and SMC (r_p = 48p =.001) (Fig. 3**E**) and MT+ and DLPFC (r_p =.45p =.002) (Fig. 3**F**).

Lastly, exploratory linear mediation analyses were conducted to

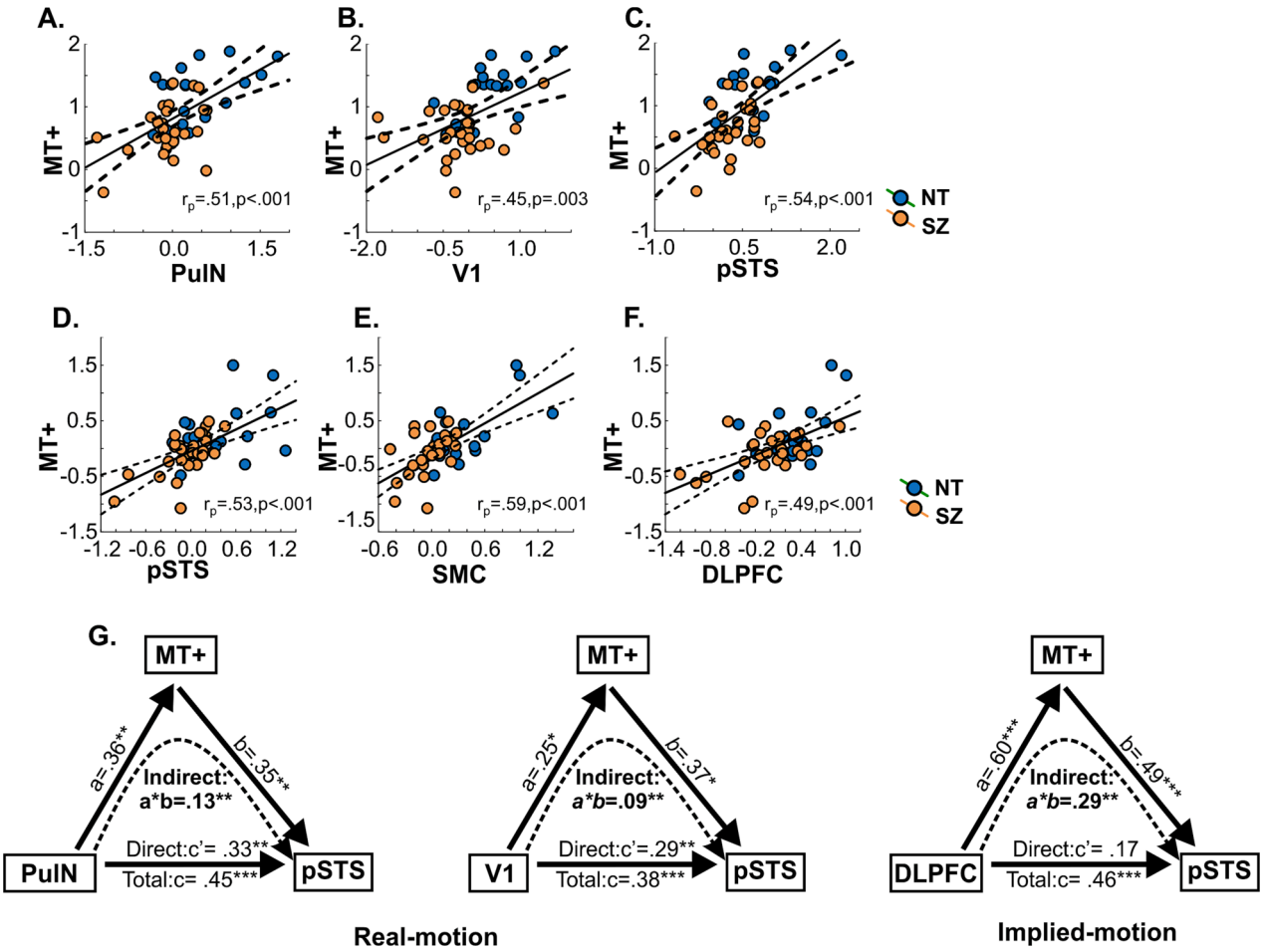

Fig. 3. Scatterplots depicting correlation between mean MT+ activation in the real-motion contrast and activation of A) pulvinar (PulN) B) V1 and C) posterior superior temporal sulcus (pSTS) for NT (blue) and SZ (orange) participants. D) Scatterplots showing correlation between MT+ activation in the implied-motion contrast and pSTS, E) sensorimotor cortex (SMC) and F) dorsolateral prefrontal cortex (DLPFC). Partial correlation coefficients (controlling for group membership, participant age, sex and IQ) and adjusted p-values are shown in each plot. G) Schematic illustration of mediation models. In all cases, MT+ was the intervening (M, mediating) variable and pSTS was the dependent (Y, outcome) variable. In the real-motion models (left and center), the independent (X, predictor) variables were PulN and V1 activation, respectively. In the implied-motion model (right), DLPFC served as the independent variable. Beta coefficient values (b) are given for the a- (X-M), b- (M−Y), c'- (direct, X-Y) and a*b- (indirect, X-Y through M) paths as well as the total (c) effect of X on Y. Significance values are denoted as: *, p <.05; **, p <.01; ***, p <.001. (For interpretation of the references to color in this figure legend, the reader is referred to the web version of this article.)

evaluate a-priori hypotheses regarding the involvement of pSTS in real- and implied-motion processing and the mediating role of MT +. Based on the correlations reported above, four predictor-outcome paths were evaluated, PulN-pSTS and V1-pSTS during real-motion and SMC-pSTS and DLPFC-pSTS during implied-motion. In all models MT+ was used as a potential mediator and sex, age, IQ and group membership as covariates.

In the real-motion condition, the (indirect) path between V1 and pSTS (b = 0.09, standard error (SE) = 0.05, 95 % CI = [0.01 0.20]) and PulN and pSTS (b = 0.13, SE = 0.06, 95 % CI = [0.03 to 0.27]) (Fig. 3**G**) was significantly mediated by MT+ (Supplementary Table 4**)**. In both models, however, the direct paths V1-pSTS (b = 0.28, SE = 0.09, 95 % CI = [0.10 0.46]) and PulN-pSTS (b = 0.33, SE = 0.11, 95 % CI = [0.10 0.55]) remained significant after controlling for MT+ activity, indicating that MT+ acted only as a partial mediator.

By contrast, in the implied-motion condition, the coefficient for the indirect path between DLPFC and pSTS was significant (b = 0.29, SE = 0.12, 95 % CI = [0.08 0.55], whereas the coefficient for their direct relationship was no longer significant after controlling for MT+ activity (b = 0.17, SE = 0.13, 95 % CI = [-0.10 0.43]) (Fig. 3**G**), consistent with full mediation.

MT+ did not mediate the association between SMC and pSTS activity (indirect path: b = 0.22, SE = 0.21, 95 % CI = [-0.24 0.59]).

3.6. *Behavioral correlations*

After controlling for group membership, participant age, sex and IQ, behavioral measures of motion-sensitivity and MT+ activation in the real-motion contrast were significantly correlated (r_p =.39, p =.008). This relationship was independently significant in the Sz group (r_p =.46, p =.020) such that reduced MT+ activity predicted poor motion sensitivity (Fig. 4**A**).

Additionally, across participants (r_p =.54,p <.001), and in Sz alone (r_p =.59, p =.002) (Fig. 4**B**), poor FER (reduced ER-40 scores) were predicted by reduced DLPFC activation during implied-motion perception.

Lastly, in Sz, symptom severity as measured by the PANSS negative syndrome scale correlated with impaired SPL activation (r_p = -0.52, p =.006) (Fig. 4**C**).

A schematic summary of the interrelationship between behavioral and fMRI measures of real- and implied-motion perception is shown in Fig. 4**D**.

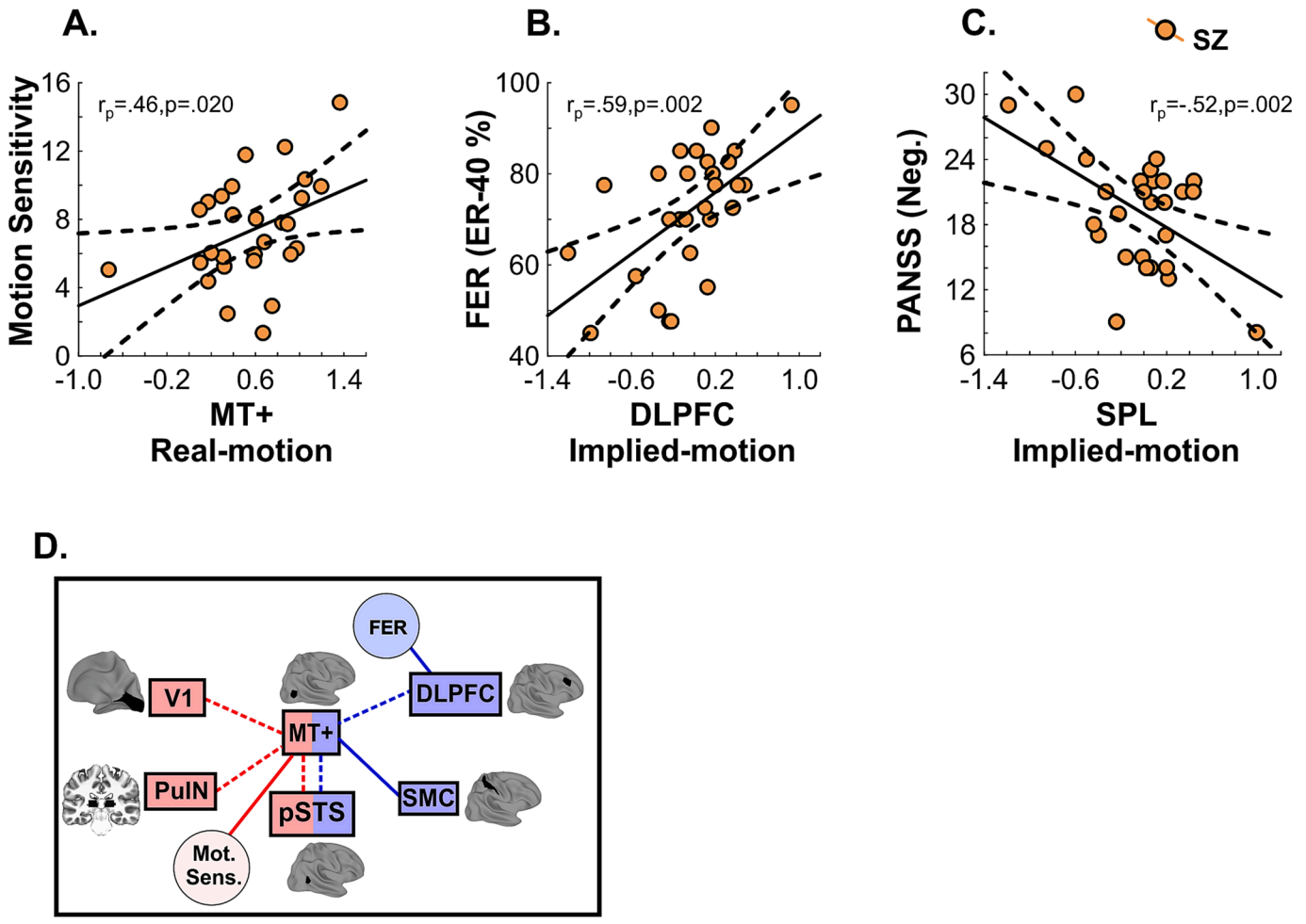

Fig. 4. A) Scatterplot showing correlation between MT+ activation during real-motion processing and motion-sensitivity score (1/threshold, derived from coherent motion detection paradigm), in Sz participants. B) Correlation of dorsolateral prefrontal cortex (DLPFC) activation to implied-motion stimuli and performance (percent correct) on ER-40 test of face emotion recognition (FER). C) Correlation between symptom severity (PANSS negative symptoms score) and activation of superior parietal lobe (SPL). Partial correlation coefficients (controlling for participant age, sex and IQ) and associated p-values are given. D) Schematic representation of the interrelationship between behavioral measures of motion sensitivity (Mot. Sens.) and FER and areas with significant group differences during real-motion (red boxes) and implied-motion (blue boxes) processing. Solid lines indicate relationships derived from correlational analyses. Dashed lines indicate putative relationship based on mediation analyses. MT+ and posterior superior temporal sulcus (pSTS) were commonly activated by real and implied-motion stimuli and, in both cases, were strongly linked with one another suggesting a possible bridging role for MT +. (For interpretation of the references to color in this figure legend, the reader is referred to the web version of this article.)

4. Discussion

Impaired motion perception is one of the most replicated examples of visual dysfunction in Sz (Chen, 2011; Hong et al., 2005; Kim et al., 2006; Li, 2002; Martinez et al., 2018) and has been shown to involve reduced activation of visual sensory regions, including MT+ (Chen et al., 2008; Lencer et al., 2005; Martinez et al., 2018). In recent years, there has been increasing appreciation of the link between the visual motion system and social brain networks (Guterstam and Graziano, 2020; Landsiedel et al., 2022; Pavlova, 2012). In particular, it has been proposed that area MT+ is a key component of an anatomically segregated pathway specialized for social cognition (Pitcher and Ungerleider, 2021). The third visual pathway transmits visual information from early sensory visual processing areas to the STS, with MT+ acting as a critical intermediary and potentially serving as a 'bridge' that links visual-sensory functions with higher-order cognitive regions (Yeo et al., 2011).

Here, we investigated the role of MT+ dysfunction in Sz in relation to functioning of the third visual pathway and the human MNS. The MNS plays a crucial role in mentalization processes, aiding in the interpretation of visual stimuli, and has been implicated in neurocognitive impairments observed across various neuropsychiatric disorders. Neural activity elicited by naturalistic stimuli consisting of real-motion video clips was compared to that elicited by static images which depicted either implied- or no-motion. We provide the first demonstration that, relative to control subjects, both MT+ and pSTS activation is reduced in Sz during both implicit- and explicit-motion perception, with a strong correlation between the two sets of deficits. Further, our data suggests that MT+ may mediate input to pSTS from both early visual (V1) and high-order (DLPFC) regions supporting concepts of MT+ as a link between purely sensory and higher-order cognitive functions (Yeo et al., 2011), and thus as a potential specific target for therapeutic intervention.

4.1. Real-motion

Cortical activity elicited by the contrast of real-motion with no-motion stimuli was localized within third visual pathway regions (V1, MT+, pSTS) and subcortically in the PulN. In all cases, activation levels were significantly lower in Sz participants, consistent with our previous findings using simple motion stimuli (Martinez et al., 2019) and dynamic emotional faces (Martínez et al., 2022). Here, we now show that these deficits extend as well to naturalistic moving scenes. In addition,

and also consistent with our prior investigation (Martinez et al., 2018), reduced motion-perception sensitivity in Sz, as measured behaviorally, correlated with diminished activation in MT +.

4.2. Implied-motion

As in previous investigations (Fawcett et al., 2007; Kourtzi and Kanwisher, 2000; Krekelberg et al., 2005; Proverbio et al., 2009; Senior et al., 2000), MT+ exhibited greater activation when participants viewed static images containing cues of implied motion compared to static images suggesting an absence of motion. Activity in pSTS was also greater for implied- versus no-motion stimuli and, like MT+, was reduced in participants with Sz.

Several cortical and subcortical nodes of the human MNS (Mineo et al., 2018; Proverbio et al., 2009; Urgesi et al., 2006) were also activated during perception of implied-motion. However, Sz participants showed reduced activity in only a subset of these including the superior parietal lobe, primary sensorimotor, DLPFC and putamen. Activation of other MNS regions, such as premotor and supplementary motor areas, were not significantly different between groups, suggesting that the observed reductions do not reflect global malfunction of the MNS, but rather abnormalities of specific subcomponents that may contribute differentially to visual perceptual functioning in Sz.

In the present study, reduced DLPFC activation during implied-motion bridged between reduced MT+ activity and FER accuracy in Sz. These findings parallel our prior observations that when a simple visual motion stimulus was used to elicit MT+ activation, MT+ activity correlated directly with FER accuracy (Martinez et al., 2018), but when a dynamic emotional face stimulus was used, pSTS served as the intervening region (Martínez et al., 2022). The MNS and superior temporal regions are known to play synergistic roles in FER (Bonini et al., 2022) and our findings suggest that both may interact with MT+ to process the explicit and/or implied-motion information needed for accurate FER determination.

Further, our finding of the mediating role of MT+ between pSTS and DLPFC lends support to the hypothesis that the involvement of MT+ in implied-motion perception is the result of feedback (modulatory) projections onto MT+ following object recognition processes in higher-level areas (Kourtzi and Kanwisher, 2000; Lorteije et al., 2006; Senior et al., 2000). Consequently, our data suggests that, in Sz, these modulatory interactions are abnormal, suggesting that developmental disruptions in MT+ organization may undermine processing across cortical networks. Together, these data suggest that developmental disruptions in MT+ organization may undermine processing across cortical networks and, if confirmed, argue for greater focus on MT+ contributions to social cognitive processing in addition to its well-documented role in visual motion processing.

Lastly, reduced SPL activation was associated with greater negative symptoms in the patient group, in agreement with prior studies (Schilbach et al., 2016; Thakkar et al., 2014) and in support of the hypotheses that a dysfunctional MNS may underlie some cognitive deficits in Sz.

4.3. Third visual pathway

For over 30 years, the prevailing model of visual system functional organization has proposed the existence of two segregated visual streams (Goodale and Milner, 1992), the dorsal ("where") and ventral ("what") pathways involved in various facets of visual object recognition. Recently the two-pathway model has been expanded to include a third pathway with cortico-cortical connections independent from those of the dorsal and ventral streams. This third pathway leads from V1 to pSTS via MT+ and is proposed to differentially processes information relevant to social cognition (Pitcher and Ungerleider, 2021). In addition to visual processing deficits previously observed in the canonical dorsal/ventral streams (reviewed in Deng et al., 2019; Javitt and Freedman, 2015)the present study adds to an accumulating literature (Martínez et al., 2022; Patel et al., 2023) demonstrating dysfunction of the third visual pathway in Sz during both real- and implicit-motion processing. Given the increasing focus on social cognition deficits as a critical determinant of functional outcome not only in Sz (Green et al., 2019; Javitt, 2023) but also in disorders such as autism (Sasson et al., 2020), future studies on the causes and consequences of third visual pathway dysfunction are warranted.

Several limitations of this study must be acknowledged. First, we showed correlations between prefrontal activation and ER-40, a normed task for the assessment of FER. In contrast, no normed tasks were available for the detection of implied-motion. Future studies with a wider array of stimuli and comprehensive behavioral measures are warranted. Second, while deficits did not correlate with medication dose, all Sz participants were receiving antipsychotics which may have affected the between-group results. Finally, although differences between groups were statistically robust, they require replication in larger samples.

5. Conclusions

Motion-processing deficits are a hallmark of Sz and have been linked to impairments in higher-order social cognitive processes. To date, deficits in MT+ activation have been investigated primarily with simple stimuli such as moving dots displays. Here, we show that MT+ deficits are also observed when motion is embedded within complex scenes and are associated with third visual pathway functioning with input from V1 and PulN to pSTS. Additionally, MT+ dysfunction in Sz was also observed in response to static images with implied-motion. In this case, the deficits were associated with a wider network involving sensorimotor and prefrontal nodes of the human MNS. The intercorrelated deficits in MT+ activation to both real- and implied-motion processing argue for a critical role for MT+ in bridging between sensory and high-order processes during visual perception in Sz.

CRediT authorship contribution statement

Antígona Martínez: Conceptualization, Formal analysis, Investigation, Methodology, Supervision, Writing – original draft, Writing – review & editing. **Pablo A. Gaspar:** Formal analysis, Investigation, Methodology. **Dalton H. Bermudez:** Formal analysis. **M. Belen Aburto-Ponce:** Formal analysis, Investigation, Supervision. **Odeta Beggel:** Project administration. **Daniel C. Javitt:** Conceptualization, Project administration, Supervision, Writing – original draft, Writing – review & editing.

Declaration of competing interest

The authors declare that they have no known competing financial interests or personal relationships that could have appeared to influence the work reported in this paper.

Data availability

Data will be made available on request.

Acknowledgements

The authors thank the Clinical Research and Evaluation Facility at NKI and all research participants for their contributions. This work was supported by National Institute of Mental Health (grant number MH49334).

Appendix A. Supplementary data

Supplementary data to this article can be found online at https://doi.org/10.1016/j.nicl.2024.103570.

References

Allison, T., Puce, A., McCarthy, G., 2000. Social perception from visual cues: role of the STS region. Trends Cogn Sci 4, 267–278.

Ammons, R., Ammons, C., 1962. The Quick Test (QT): provisional manual. Psychol. Rep. 11, 111–162.

Andreasen, N.C., Pressler, M., Nopoulos, P., Miller, D., Ho, B.C., 2010. Antipsychotic dose equivalents and dose-years: a standardized method for comparing exposure to different drugs. Biol Psychiatry 67, 255–262.

Bonini, L., 2017. The extended mirror neuron network: anatomy, origin, and functions. Neuroscientist 23, 56–67.

Bonini, L., Rotunno, C., Arcuri, E., Gallese, V., 2022. Mirror neurons 30 years later: implications and applications. Trends Cogn Sci 26, 767–781.

Brown, E.C., Gonzalez-Liencres, C., Tas, C., Brune, M., 2016. Reward modulates the mirror neuron system in schizophrenia: a study into the mu rhythm suppression, empathy, and mental state attribution. Soc Neurosci 11, 175–186.

Caspers, S., Zilles, K., Laird, A.R., Eickhoff, S.B., 2010. ALE meta-analysis of action observation and imitation in the human brain. Neuroimage 50, 1148–1167.

Chan, M.M.Y., Han, Y.M.Y., 2020. Differential mirror neuron system (MNS) activation during action observation with and without social-emotional components in autism: a meta-analysis of neuroimaging studies. Mol Autism 11, 72.

Chen, Y., 2011. Abnormal visual motion processing in schizophrenia: a review of research progress. Schizophr Bull 37, 709–715.

Chen, Y., Grossman, E.D., Bidwell, L.C., Yurgelun-Todd, D., Gruber, S.A., Levy, D.L., Nakayama, K., Holzman, P.S., 2008. Differential activation patterns of occipital and prefrontal cortices during motion processing: evidence from normal and schizophrenic brains. Cogn Affect Behav Neurosci 8, 293–303.

Choe, E., Lee, T.Y., Kim, M., Hur, J.W., Yoon, Y.B., Cho, K.K., Kwon, J.S., 2018. Aberrant within- and between-network connectivity of the mirror neuron system network and the mentalizing network in first episode psychosis. Schizophr Res 199, 243–249.

Choi, E.Y., Yeo, B.T., Buckner, R.L., 2012. The organization of the human striatum estimated by intrinsic functional connectivity. J Neurophysiol 108, 2242–2263.

Cox, R.W., 1996. AFNI - Software for analysis and visualization of functional magnetic resonance neuroimages. Comput. Biomed. Res. 29, 162–173.

Deng, Y., Liu, K., Cheng, D., Zhang, J., Chen, H., Chen, B., Li, Y., Wang, W., Kong, Y., Wen, G., 2019. Ventral and dorsal visual pathways exhibit abnormalities of static and dynamic connectivities, respectively, in patients with schizophrenia. Schizophr Res 206, 103–110.

Errante, A., Fogassi, L., 2020. Activation of cerebellum and basal ganglia during the observation and execution of manipulative actions. Sci Rep 10, 12008.

Fawcett, I.P., Hillebrand, A., Singh, K.D., 2007. The temporal sequence of evoked and induced cortical responses to implied-motion processing in human motion area V5/MT+. Eur J Neurosci 26, 775–783.

Ferrari, P.F., Gerbella, M., Coude, G., Rozzi, S., 2017. Two different mirror neuron networks: the sensorimotor (hand) and limbic (face) pathways. Journal of 358, 300–315.

Filimon, F., Nelson, J.D., Hagler, D.J., Sereno, M.I., 2007. Human cortical representations for reaching: mirror neurons for execution, observation, and imagery. Neuroimage 37, 1315–1328.

First, M.B., Spitzer, R.L., Gibbon, M., Williams, J.B.W., 1997. Structured Clinical Interview for DSM-IV Axis I Disorders- Patient Edition. New York State Psychiatric Institute, New York.

Glasser, M.F., Coalson, T.S., Robinson, E.C., Hacker, C.D., Harwell, J., Yacoub, E., Ugurbil, K., Andersson, J., Beckmann, C.F., Jenkinson, M., Smith, S.M., Van Essen, D. C., 2016. A multi-modal parcellation of human cerebral cortex. Nature 536, 171–178.

Goodale, M.A., Milner, A.D., 1992. Separate visual pathways for perception and action. Trends Neurosci 15, 20–25.

Green, M.F., Horan, W.P., Lee, J., 2019. Nonsocial and social cognition in schizophrenia: current evidence and future directions. World Psychiatry 18, 146–161.

Guterstam, A., Graziano, M.S.A., 2020. Visual motion assists in social cognition. Proc Natl Acad Sci U S A 117, 32165–32168.

Hayes, A.F., 2013. Introduction to mediation, moderation, and conditional process analysis : a regression-based approach. The Guilford Press, New York.

Hong, L.E., Tagamets, M., Avila, M., Wonodi, I., Holcomb, H., Thaker, G.K., 2005. Specific motion processing pathway deficit during eye tracking in schizophrenia: a performance-matched functional magnetic resonance imaging study. Biol Psychiatry 57, 726–732.

Jarrett, C.B., Phillips, M., Parker, A., Senior, C., 2002. Implicit motion perception in schizotypy and schizophrenia: a representational momentum study. Cogn Neuropsychiatry 7, 1–14.

Javitt, D.C., 2023. Cognitive impairment associated with schizophrenia: from pathophysiology to treatment. Annu Rev Pharmacol Toxicol 63, 119–141.

Javitt, D.C., Freedman, R., 2015. Sensory processing dysfunction in the personal experience and neuronal machinery of schizophrenia. Am J Psychiatry 172, 17–31.

Jeon, H., Lee, S.H., 2018. From neurons to social beings: short review of the mirror neuron system research and its socio-psychological and psychiatric implications. Clin Psychopharmacol Neurosci 16, 18–31.

Ji, J.L., Spronk, M., Kulkarni, K., Repovs, G., Anticevic, A., Cole, M.W., 2019. Mapping the human brain's cortical-subcortical functional network organization. Neuroimage 185, 35–57.

Kelemen, O., Erdelyi, R., Pataki, I., Benedek, G., Janka, Z., Keri, S., 2005. Theory of mind and motion perception in schizophrenia. Neuropsychology 19, 494–500.

Kim, D., Wylie, G., Pasternak, R., Butler, P.D., Javitt, D.C., 2006. Magnocellular contributions to impaired motion processing in schizophrenia. Schizophr Res 82, 1–8.

Kourtzi, Z., Kanwisher, N., 2000. Activation in human MT/MST by static images with implied motion. J. Cogn. Neurosci. 12, 48–55.

Krekelberg, B., Vatakis, A., Kourtzi, Z., 2005. Implied motion from form in the human visual cortex. J Neurophysiol 94, 4373–4386.

Kriegeskorte, N., Simmons, W.K., Bellgowan, P.S., Baker, C.I., 2009. Circular analysis in systems neuroscience: the dangers of double dipping. Nat Neurosci 12, 535–540.

Kronbichler, L., Tschernegg, M., Martin, A.I., Schurz, M., Kronbichler, M., 2017. Abnormal brain activation during theory of mind tasks in schizophrenia: a meta-analysis. Schizophr Bull 43, 1240–1250.

LaBar, K.S., Crupain, M.J., Voyvodic, J.T., McCarthy, G., 2003. Dynamic perception of facial affect and identity in the human brain. Cereb. Cortex 13, 1023–1033.

Landsiedel, J., Daughters, K., Downing, P.E., Koldewyn, K., 2022. The role of motion in the neural representation of social interactions in the posterior temporal cortex. Neuroimage 262, 119533.

Lencer, R., Nagel, M., Sprenger, A., Heide, W., Binkofski, F., 2005. Reduced neuronal activity in the V5 complex underlies smooth-pursuit deficit in schizophrenia: evidence from an fMRI study. Neuroimage 24, 1256–1259.

Li, C.S., 2002. Impaired detection of visual motion in schizophrenia patients. Prog Neuropsychopharmacol Biol Psychiatry 26, 929–934.

Lorteije, J.A., Kenemans, J.L., Jellema, T., van der Lubbe, R.H., de Heer, F., van Wezel, R. J., 2006. Delayed response to animate implied motion in human motion processing areas. J. Cogn. Neurosci. 18, 158–168.

Martínez, A., Tobe, R.H., Gaspar, P.A., Malinsky, D., Dias, E.C., Sehatpour, P., Lakatos, P., Patel, G.H., Bermudez, D.H., Silipo, G., Javitt, D.C., 2022. Disease-Specific Contribution of Pulvinar Dysfunction to Impaired Emotion Recognition in Schizophrenia. Front Behav Neurosci 15.

Martinez, A., Gaspar, P.A., Hillyard, S.A., Andersen, S.K., Lopez-Calderon, J., Corcoran, C.M., Javitt, D.C., 2018. Impaired motion processing in schizophrenia and the attenuated psychosis syndrome: etiological and clinical implications. Am J Psychiatry 175, 1243–1254.

Martinez, A., Tobe, R., Dias, E.C., Ardekani, B.A., Veenstra-VanderWeele, J., Patel, G., Breland, M., Lieval, A., Silipo, G., Javitt, D.C., 2019. Differential patterns of visual sensory alteration underlying face emotion recognition impairment and motion perception deficits in schizophrenia and autism spectrum disorder. Biol Psychiatry 86, 557–567.

Matsumoto, Y., Takahashi, H., Miyata, J., Sugihara, G., Murai, T., Takahashi, H., 2018. Neural basis of altered earlier attention and higher order biological motion processing in schizophrenia. Soc Neurosci 13, 594–601.

Mehta, U.M., Thirthalli, J., Aneelraj, D., Jadhav, P., Gangadhar, B.N., Keshavan, M.S., 2014a. Mirror neuron dysfunction in schizophrenia and its functional implications: a systematic review. Schizophr Res 160, 9–19.

Mehta, U.M., Thirthalli, J., Basavaraju, R., Gangadhar, B.N., Pascual-Leone, A., 2014b. Reduced mirror neuron activity in schizophrenia and its association with theory of mind deficits: evidence from a transcranial magnetic stimulation study. Schizophr Bull 40, 1083–1094.

Mier, D., Eisenacher, S., Rausch, F., Englisch, S., Gerchen, M.F., Zamoscik, V., Meyer-Lindenberg, A., Zink, M., Kirsch, P., 2017. Aberrant activity and connectivity of the posterior superior temporal sulcus during social cognition in schizophrenia. Eur Arch Psychiatry Clin Neurosci 267, 597–610.

Mineo, L., Fetterman, A., Concerto, C., Warren, M., Infortuna, C., Freedberg, D., Chusid, E., Aguglia, E., Battaglia, F., 2018. Motor facilitation during observation of implied motion: evidence for a role of the left dorsolateral prefrontal cortex. Int J Psychophysiol 128, 47–51.

Molenberghs, P., Cunnington, R., Mattingley, J.B., 2012. Brain regions with mirror properties: a meta-analysis of 125 human fMRI studies. Neurosci. Biobehav. Rev. 36, 341–349.

Okruszek, L., Pilecka, I., 2017. Biological motion processing in schizophrenia - systematic review and meta-analysis. Schizophr Res 190, 3–10.

Osaka, N., Matsuyoshi, D., Ikeda, T., Osaka, M., 2010. Implied motion because of instability in Hokusai Manga activates the human motion-sensitive extrastriate visual cortex: an fMRI study of the impact of visual art. Neuroreport 21, 264–267.

Patel, G.H., Gruskin, D.C., Arkin, S.C., Jamerson, E.C., Ruiz-Betancourt, D.R., Klim, C.C., Sanchez-Pena, J.P., Bartel, L.P., Lee, J.K., Grinband, J., Martinez, A., Berman, R.A., Ochsner, K.N., Leopold, D.A., Javitt, D.C., 2023. The road not taken: disconnection of a human-unique cortical pathway underlying naturalistic social perception in schizophrenia. Biol Psychiatry Glob Open Sci 3, 398–408.

Pavlova, M.A., 2012. Biological motion processing as a hallmark of social cognition. Cereb. Cortex 22, 981–995.

Pitcher, D., Ungerleider, L.G., 2021. Evidence for a third visual pathway specialized for social perception. Trends Cogn Sci 25, 100–110.

Preacher, K.J., Hayes, A.F., 2008. Asymptotic and resampling strategies for assessing and comparing indirect effects in multiple mediator models. Behav Res Methods 40, 879–891.

Proverbio, A.M., Riva, F., Zani, A., 2009. Observation of static pictures of dynamic actions enhances the activity of movement-related brain areas. PLoS One 4, e5389.

Saad, Z.S., Reynolds, R.C., 2012. Suma. Neuroimage 62, 768–773.

Saito, Y., Kubicki, M., Koerte, I., Otsuka, T., Rathi, Y., Pasternak, O., Bouix, S., Eckbo, R., Kikinis, Z., von Hohenberg, C.C., Roppongi, T., Del Re, E., Asami, T., Lee, S.H., Karmacharya, S., Mesholam-Gately, R.I., Seidman, L.J., Levitt, J., McCarley, R.W., Shenton, M.E., Niznikiewicz, M.A., 2018. Impaired white matter connectivity between regions containing mirror neurons, and relationship to negative symptoms and social cognition, in patients with first-episode schizophrenia. Brain Imaging Behav 12, 229–237.

Sasson, N.J., Morrison, K.E., Kelsven, S., Pinkham, A.E., 2020. Social cognition as a predictor of functional and social skills in autistic adults without intellectual disability. Autism Res 13, 259–270.

Scheliga, S., Schwank, R., Scholle, R., Habel, U., Kellermann, T., 2022. A neural mechanism underlying predictive visual motion processing in patients with schizophrenia. Psychiatry Res 318, 114934.
Schilbach, L., Derntl, B., Aleman, A., Caspers, S., Clos, M., Diederen, K.M., Gruber, O., Kogler, L., Liemburg, E.J., Sommer, I.E., Muller, V.I., Cieslik, E.C., Eickhoff, S.B., 2016. Differential patterns of dysconnectivity in mirror neuron and mentalizing networks in schizophrenia. Schizophr Bull 42, 1135–1148.
Schmidt, S.N.L., Hass, J., Kirsch, P., Mier, D., 2021. The human mirror neuron system-a common neural basis for social cognition? Psychophysiology 58, e13781.
Senior, C., Barnes, J., Giampietro, V., Simmons, A., Bullmore, E.T., Brammer, M., David, A.S., 2000. The functional neuroanatomy of implicit-motion perception or representational momentum. Curr Biol 10, 16–22.
Taylor, S.F., MacDonald, A.W., 3rd, Cognitive Neuroscience Treatment Research to Improve Cognition in, S., 2012. Brain mapping biomarkers of socio-emotional processing in schizophrenia. Schizophr Bull 38, 73-80.
Taylor, P.A., Chen, G., Glen, D.R., Rajendra, J.K., Reynolds, R.C., Cox, R.W., 2018. FMRI processing with AFNI: Some comments and corrections on “Exploring the Impact of Analysis Software on Task fMRI Results”. bioRXiv https://doi.org/10.1101/308643.
Thakkar, K.N., Peterman, J.S., Park, S., 2014. Altered brain activation during action imitation and observation in schizophrenia: a translational approach to investigating social dysfunction in schizophrenia. Am J Psychiatry 171, 539–548.
Urgesi, C., Moro, V., Candidi, M., Aglioti, S.M., 2006. Mapping implied body actions in the human motor system. J. Neurosci. 26, 7942–7949.
Valizadeh, A., Mbwogge, M., Rasouli Yazdi, A., Hedayati Amlashi, N., Haadi, A., Shayestefar, M., Moassefi, M., 2022. The mirror mechanism in schizophrenia: a systematic review and qualitative meta-analysis. Front Psychiatry 13, 884828.
Willenbockel, V., Sadr, J., Fiset, D., Horne, G.O., Gosselin, F., Tanaka, J.W., 2010. Controlling low-level image properties: the SHINE toolbox. Behav Res Methods 42, 671–684.
Yeo, B.T., Krienen, F.M., Sepulcre, J., Sabuncu, M.R., Lashkari, D., Hollinshead, M., Roffman, J.L., Smoller, J.W., Zollei, L., Polimeni, J.R., Fischl, B., Liu, H., Buckner, R. L., 2011. The organization of the human cerebral cortex estimated by intrinsic functional connectivity. J Neurophysiol 106, 1125–1165.
Zeki, S., Watson, J.D., Frackowiak, R.S., 1993. Going beyond the information given: the relation of illusory visual motion to brain activity. Proc Biol Sci 252, 215–222.
Zhang, D., Snyder, A.Z., Fox, M.D., Sansbury, M.W., Shimony, J.S., Raichle, M.E., 2008. Intrinsic functional relations between human cerebral cortex and thalamus. J Neurophysiol 100, 1740–1748.